

TABLE II
COMPARISON OF SHORT-CIRCUIT POWER DISSIPATION
FORMULAE WITH SPICE SIMULATION RESULTS

C _L (pF)	rise time (ns)	fall time (ns)	W _T (μm)		Short circuit power dissipation (μW)					SPICE
			PMOS	NMOS	(1) & (2) of [7]	(11) of [9]	(10) of [4]	eqn (12)		
0.15	5	5	4.8/1.2	4.8/1.2	47.1	141.1	63.5	21.56	18.49	
0.15	2	2	4.8/1.2	4.8/1.2	13.35	56.44	25.4	4.24	4.08	
0.30	5	5	4.8/1.2	4.8/1.2	36.56	141.1	63.5	12.85	14.26	
0.15	5	5	9.6/1.2	9.6/1.2	115.30	284.7	127.1	65.60	43.62	
0.30	2	2	9.6/1.2	9.6/1.2	26.70	113.9	50.8	8.61	6.81	
0.15	5	5	4/1	4/1	54.18	166.5	70.55	31.95	26.29	
0.15	2	2	4/1	4/1	15.47	66.59	28.22	6.52	7.32	
0.30	5	5	4/1	4/1	41.5	166.5	70.55	19.58	20.50	
0.15	5	5	8/1	8/1	131.58	336.4	141.11	94.35	43.62	
0.30	2	2	8/1	8/1	30.94	134.5	56.44	13.28	15.65	
0.15	5	5	3.2/0.8	3.2/0.8	68.65	222.8	84.70	65.12	47.19	
0.15	2	2	3.2/0.8	3.2/0.8	20.00	89.13	33.88	14.59	13.06	
0.30	5	5	3.2/0.8	3.2/0.8	54.44	42.87	84.70	42.87	40.00	
0.15	5	5	6.4/0.8	6.4/0.8	164.85	180.46	169.40	149.77	118.8	
0.30	2	2	6.4/0.8	6.4/0.8	39.99	29.77	67.76	29.78	27.01	

TABLE III
COMPARISON OF SHORT-CIRCUIT POWER DISSIPATION AND
DYNAMIC POWER DISSIPATION RESULTS OF CMOS LOGIC GATES

Gate	C _L (pF)	rise time (ns)	Gate length (μm)	2 input NAND					%P _{sc} P _{sc}
				P _d SPICE	# of active p-FETs	P _{sc}			
						SPICE	eqn (12)	% error	
NAND2	0.15	5	0.8	94.9	1	37.41	24.96	33.3	39.4
				104.9	2	42.55	39.02	8.3	40.6
NAND2	0.15	5	1.0	114.1	2	35.00	37.22	6.3	30.7
NAND2	0.15	5	1.2	128.0	2	28.64	36.51	27.4	21.4
NAND2	0.30	2	0.8	179.6	2	7.04	3.55	49.5	3.9
NAND2	0.30	2	1.0	186.1	2	5.66	3.42	60.4	3.0
NAND3	0.15	5	0.8	101.2	1	32.59	16.38	49.7	32.2
				108.9	2	39.44	25.48	35.4	36.2
				115.6	3	41.86	32.89	21.5	36.3
NAND3	0.15	5	1.0	135.6	3	33.54	31.60	5.8	24.7
NAND3	0.15	5	1.2	135.7	2	24.72	24.30	1.7	17.9
NAND3	0.30	2	0.8	190.6	3	3.00	1.97	34.4	1.6
NAND3	0.30	2	1.0	206.9	3	3.95	2.13	46.1	1.9

larger in case of NAND gates because the effect of source/drain capacitances in the chain of serially-connected NMOSFETs is neglected in obtaining an equivalent inverter. With reducing channel lengths of NMOSFETs the ratio of short-circuit power dissipation to dynamic power dissipation increases as seen in last column of Table III. This indicates that the short-circuit power dissipation becomes more significant in short-channel transistors. P_{sc} contribution to total power dissipation also increases with supply voltage scaling since the threshold voltage of MOSFETs does not scale down proportionally to supply voltages [1].

With reducing values of supply voltages and channel lengths in CMOS circuits, short circuit current contribution towards overall power dissipation is increasing. Therefore there is a need for simple but accurate formula for estimating short-circuit power dissipation. Though the proposed formula for short-circuit power dissipation takes more computations than the formulae used by Veendrick and Sakurai, it includes additional effects ignored by these formulae and hence more accurate. Comparing with (1) and (2) of [7], the

proposed formula takes less computation time and is more accurate in estimating short-circuit power dissipation. This difference becomes even more apparent in the case of short-channel MOS transistor circuits.

REFERENCES

- [1] A. P. Chandrakasan, S. Sheng, and R. W. Brodersen, "Low-power CMOS digital design," *IEEE J. Solid-State Circuits*, vol. 27, pp. 473-484, Apr. 1992.
- [2] D. Liu and C. Svensson, "Trading speed for low power by choice of supply and threshold voltages," *IEEE J. Solid-State Circuits*, vol. 28, pp. 10-17, Jan. 1993.
- [3] P. S. P. Vanoostende, P. Six, J. Vandewalle, and H. J. De Man, "Estimation of typical power of synchronous CMOS circuits using a hierarchy of simulator," *IEEE J. Solid-State Circuits*, vol. 28, pp. 26-39, Jan. 1993.
- [4] H. J. M. Veendrick, "Short-circuit power dissipation of static CMOS circuitry and its impact on the design of buffer circuits," *IEEE J. Solid-State Circuits*, vol. SC-19, pp. 468-473, Aug. 1984.
- [5] N. Hedenstierna and K. Jeppson, "CMOS circuit speed and buffer optimization," *IEEE Trans. CAD*, vol. 6, pp. 270-281, Mar. 1987.
- [6] A. J. Al-Khalili, Y. Zhu, and D. Al-Khalili, "A module generator for optimized CMOS buffers," *IEEE Trans. CAD*, vol. 9, pp. 1028-1046, Oct. 1990.
- [7] N. Hedenstierna and K. Jeppson, "Comments on 'A module generator for optimized CMOS buffers'," *IEEE Trans. CAD*, vol. 12, pp. 180-181, Jan. 1993.
- [8] H. Shichman and D. A. Hodges, "Modeling and simulation of insulated-gate field-effect transistor switching circuits," *IEEE J. Solid-State Circuits*, vol. SC-3, pp. 28-289, Sept. 1968.
- [9] T. Sakurai and A. Newton, "Alpha-power law MOSFET model and its applications to CMOS inverter delay and other formulas," *IEEE J. Solid-State Circuits*, vol. 25, pp. 584-594, Apr. 1990.
- [10] S. M. Kang, "Accurate simulation of power dissipation in VLSI circuits," *IEEE J. Solid-State Circuits*, vol. SC-21, pp. 889-891, Oct. 1986.

Singularity Induced Bifurcation and the van der Pol Oscillator

Vaithianathan Venkatasubramanian

Abstract— In parameter dependent differential-algebraic models (DAEs) of the form $\dot{x} = f$ and $0 = g$, it has been shown recently that the generic codimension one local bifurcations are the well-known saddle node and Hopf bifurcations and a new bifurcation called the singularity induced bifurcation. The latter occurs generically when an equilibrium of the DAE system crosses the singular surface of noncausal points. In this paper, it is shown that when singularly perturbed models of the form $\dot{x} = f$ and $\epsilon \dot{y} = g$ are considered, the singularity induced bifurcation in the slow DAE system corresponds to oscillatory behavior in the singularly perturbed models. As an example, it is proved that the oscillations in the classical van der Pol oscillator arise when a stable equilibrium undergoes the singularity induced bifurcation in the slow DAE system, which in turn corresponds to the occurrence of supercritical Hopf bifurcations in the singularly perturbed models.

I. INTRODUCTION

A large class of physical systems such as nonlinear networks [1] can be modeled by singularly perturbed nonlinear systems of the

Manuscript received September 22, 1994; revised May 5, 1993.
The author is with the School of Electrical Engineering and Computer Science, Washington State University, Pullman, WA 99164-2752 USA.
IEEE Log Number 9405523.

form

$$\Sigma_\epsilon : \dot{x} = f(x, y, p), \quad f: \mathbb{R}^{n+m+q} \rightarrow \mathbb{R}^n, \quad f \text{ is } C^\infty \quad (1)$$

$$\epsilon \dot{y} = g(x, y, p), \quad g: \mathbb{R}^{n+m+q} \rightarrow \mathbb{R}^m, \quad g \text{ is } C^\infty \quad (2)$$

$$x \in X \subset \mathbb{R}^n, \quad y \in Y \subset \mathbb{R}^m, \quad p \in P \subset \mathbb{R}^q$$

Here the state variables x and y , respectively, denote the *slow* and *fast* states of the system Σ_ϵ , and p represents the system parameters. The *slow dynamics* Σ_s of the system Σ_ϵ can be defined as the differential-algebraic model (DAE)

$$\Sigma_s : \dot{x} = f(x, y, p) \quad (3)$$

$$0 = g(x, y, p) \quad (4)$$

Similarly the *fast system* Σ_f associated with Σ_ϵ can be defined as

$$\Sigma_f : x' = 0 \quad (5)$$

$$y' = g(x, y, p) \quad (6)$$

where x' denotes time differentiation in the fast time scale $\tau = \frac{t}{\epsilon}$. The singular perturbation theory (e.g. [2], [3]) allows us to infer the properties of the system Σ_ϵ by analyzing the subsystems Σ_s and Σ_f under certain assumptions. In particular, standard singular perturbation theory assumes that the trajectories of Σ_ϵ stay away from the singular subset S of the slow manifold L ,

$$L := \{(x, y, p) \in \mathbb{R}^{n+m+q} : g(x, y, p) = 0\} \quad (7)$$

$$S := \{(x, y, p) \in L : \Delta(x, y, p) := \det(D_y g)(x, y, p) = 0\} \quad (8)$$

where $D_y g$ denotes the matrix of partial derivatives $\frac{\partial g}{\partial y}$. The trajectories of Σ_ϵ typically undergo "jumps" upon reaching the singular surface [4], [5]. By analyzing the DAE system Σ_s , it is proved in [1] that generically most of the singular points in S consist of impasse points where the trajectories of the DAE system cannot be continued. A detailed analysis of the singular dynamics of Σ_s is presented in [6]–[8] motivated by the dynamics of the large electric power system.

In [6], it has been proved that the generic codimension one local bifurcations for the constrained system Σ_s are the well-known saddle node and Hopf bifurcations, and a new bifurcation called the singularity induced bifurcation (SIB). The singularity induced bifurcation occurs when an equilibrium of Σ_s crosses the singular set S upon parameter variation, i.e. described by the conditions

$$f(x, y, p) = 0 \quad (9)$$

$$g(x, y, p) = 0 \quad (10)$$

$$\Delta(x, y, p) = 0 \quad (11)$$

The Singularity Induced Bifurcation Theorem, which summarizes the eigenvalue analysis of this phenomenon in Σ_s , is quoted from [6] in the Appendix.

Note that in the singularly perturbed model Σ_ϵ , there is extreme complexity in analyzing the system behavior near the singularity induced bifurcation because then the equilibrium is near the singular set S , and the standard tools are not applicable there [10]. Using nonstandard analytical tools, the recent theory of canards ("duck-shooting" [10]) studies the special nature of certain oscillations (which are highly sensitive to perturbations) known as duck-cycles of Σ_ϵ in small dimensions (for $n+m \leq 4$) near certain special singular

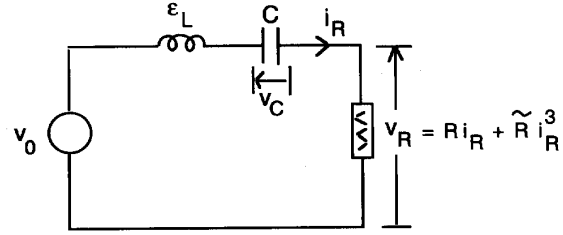


Fig. 1. Nonlinear network representation of a van der Pol oscillator.

solutions known as canards [11]. Specifically in [11], it is shown that: (1) canards must pass through the singular equilibrium points described by the conditions (9)–(11) for the case of $n = m = 1$; and (2) upon certain small perturbations of Σ_ϵ , canards lead to a rich structure of oscillatory phenomena known as canard-oscillations (or duck-solutions) via Hopf bifurcations. However the presence of canards and duck-solutions in higher dimensional systems (e.g. the results in [12] for $n = 2$ and $m = 1$) is not directly related to the conditions (9)–(11).

In this paper, using the geometric results for the slow dynamics Σ_s from [6]–[8], it will be proved that *when a stable equilibrium point of the large system Σ_ϵ crosses the singularity induced bifurcation boundary described by the conditions (9)–(11), generically the local stability at the equilibrium is lost in Σ_ϵ with two eigenvalues of the system Σ_ϵ crossing the imaginary axis.* As such, the conditions (9)–(11) do not indicate any connection to such oscillatory phenomena, but the interaction of the slow and fast dynamics of Σ_ϵ near the SIB results in the presence of purely imaginary eigenvalues as shown in Section 3.

A simple example, that of a van der Pol oscillator, is presented first in Section 2, where the birth of limit cycles at the singularity induced bifurcation is clearly illustrated. Explicit computations prove the emergence of the singularity induced bifurcation in Σ_s as the limit of Hopf bifurcations in Σ_ϵ . In Section 3, large system models are considered.

II. AN EXAMPLE OF A VAN DER POL OSCILLATOR

Consider a nonlinear resistor whose v-i characteristics are given by

$$v_R = R i_R + \tilde{R} i_R^3 \quad (12)$$

connected in series with a linear capacitor C and a voltage source v_0 . Assuming a parasitic inductance $\epsilon_L = \frac{\epsilon}{C}$ in the network, the dynamics of this simple nonlinear network shown in Fig. 1 is governed by the equations

$$C \dot{v}_C = i_R \quad (13)$$

$$\epsilon_L \dot{i}_R = v_0 - (R i_R + \tilde{R} i_R^3) - v_C \quad (14)$$

Setting $x = v_C - v_0$, $y = \frac{i_R}{C}$, $\mu_1 = RC$, and $\mu_2 = \tilde{R} C^3$, these equations can be restated as

$$\Sigma_{vP} : \dot{x} = y \quad (15)$$

$$\epsilon \dot{y} = -x - \mu_1 y - \mu_2 y^3 \quad (16)$$

The system Σ_{vP} describes a class of van der Pol oscillators (the Liénard form) which has been long studied in the literature. Recent citations include the case of jump phenomena [5] when $\mu_1 = -1$ and $\mu_2 = 1$, and the treatment of the classical van der Pol oscillator

example using the theory of relaxation oscillations in [3] with $\mu_1 = -1$ and $\mu_2 = \frac{1}{3}$. Here we will analyze the bifurcation phenomena in Σ_{vP} when the parameters μ_1 and μ_2 are varied.

First let us analyze the slow system associated with Σ_{vP} which is the DAE system Σ_1 ,

$$\Sigma_1 : \dot{x} = y \quad (17)$$

$$0 = -x - \mu_1 y - \mu_2 y^3 \quad (18)$$

The set of singular points S (8) for Σ_1 are easily seen to satisfy $\mu_1 + 3\mu_2 y^2 = 0$. So the geometry of the slow manifold L defined by (18) is that of a cusp and the system Σ_1 has two (none) singular points when $\mu_1 \mu_2 < 0$ ($\mu_1 \mu_2 > 0$). The system has a unique equilibrium point at $x = y = 0$ for all parameter values. However when $\mu_1 = 0$, this equilibrium coincides with the singular point, resulting in the singularity induced bifurcation. It is easily verified that the transversality conditions (SI1), (SI2) and (SI3') (see Appendix) are satisfied at the bifurcation and hence the only eigenvalue of the system Σ_1 must become unbounded at the SIB point $\mu_1 = 0$. For Σ_1 , this eigenvalue can be directly computed to be $-\frac{1}{\mu_1}$, so it is indeed true that when μ_1 is decreased from $0+$ to $0-$ through $\mu_1 = 0$, the eigenvalue moves from C^- to C^+ by diverging through infinity. For large systems, this eigenvalue cross-over through infinity is highly significant, as we will see in Section 3.

Next the limiting behavior of the singularly perturbed system Σ_{vP} will be analyzed for small $\epsilon > 0$ near the SIB points $\mu_1 = 0$. Specifically it will be proved that the singularity induced bifurcation in the slow system Σ_1 (with $\epsilon = 0$) for $\mu_1 = 0$ corresponds to the occurrence of Hopf bifurcations in the singularly perturbed model Σ_{vP} for $\mu_1 = 0$ when $\epsilon \neq 0$. The proof directly follows by an application of the Hopf bifurcation Theorem and the related normal form computations [13].

Note that the only equilibrium for Σ_{vP} is $x = y = 0$ and the eigenvalues (λ) at this equilibrium are the solutions of

$$\epsilon \lambda^2 + \mu_1 \lambda + 1 = 0 \quad (19)$$

Therefore the eigenvalues are purely imaginary at $\mu_1 = 0$. It will be shown next that $\mu_1 = 0$ corresponds to the occurrence of Hopf bifurcation for Σ_{vP} . To apply the Hopf bifurcation theorem [13], first the constant d can be seen from (19) to be

$$d := \frac{d}{d\mu_1|_{\mu_1=0}} \text{Real}(\lambda(\mu_1)) = -\frac{1}{2\epsilon} \quad (20)$$

For computing the normal form constant a , let us represent the system in the standard form in [13] with the linear transformation $(x_1, y_1) = (\frac{x}{\sqrt{\epsilon}}, y)$ so that Σ_{vP} at $\mu_1 = 0$ becomes

$$\begin{pmatrix} \dot{x}_1 \\ \dot{y}_1 \end{pmatrix} = \begin{pmatrix} 0 & \frac{1}{\sqrt{\epsilon}} \\ -\frac{1}{\sqrt{\epsilon}} & 0 \end{pmatrix} \begin{pmatrix} x_1 \\ y_1 \end{pmatrix} + \begin{pmatrix} 0 \\ -\frac{\mu_2}{\epsilon} y_1^3 \end{pmatrix} \quad (21)$$

Now applying the formula from [13] for the constant a , we find $a = -\frac{3\mu_2}{8\epsilon}$. Therefore the Hopf bifurcation at $\mu_1 = 0$ is supercritical when $\mu_2 > 0$ and is subcritical when $\mu_2 < 0$ for any value of $\epsilon > 0$. Also by the Hopf theorem [13], when $\mu_2 > 0$ ($\mu_2 < 0$), the stable (unstable) limit cycles appearing for $\mu_1 = 0 - (\mu_1 = 0+)$ near the origin are well-approximated in the (x_1, y_1) coordinates by

$$x_1^2 + y_1^2 = -\frac{d}{a}\mu_1 = -\frac{4}{3\mu_2}\mu_1 \quad (22)$$

Therefore in the $(x_1, y_1) = (\frac{x}{\sqrt{\epsilon}}, y)$ coordinates, the size of the limit cycles (the first order approximations) is independent of ϵ , and hence the proof that the limit cycles persist as ϵ goes to zero. In (x, y) coordinates, these limit cycles then approach the jump phenomena consisting of two slow movements along the slow manifold of Σ_1 and two jumps at the singular points in Σ_1 . Of course the nonexistence

of the limit cycles when $\mu_1 \mu_2 > 0$ can be easily proved from the Bendixon criterion, and the existence of the limit cycle for $\mu_1 \mu_2 < 0$ can also be proved using the Poincare-Bendixon Theorem as presented in textbooks (e.g. [14]).

Here we note that Hopf bifurcations in Σ_{vP} are special in the sense that as $\epsilon \rightarrow 0$, the purely imaginary eigenvalues at the bifurcation diverge to infinity, and the behavior at $\epsilon = 0+$ is not obvious. The above normal form computations prove that indeed limit cycles persist as $\epsilon \rightarrow 0$ and approach an oscillatory jump phenomenon. Moreover in the reduced system or the slow system Σ_1 , the bifurcation at $\mu_1 = 0$ is the singularity induced bifurcation with one eigenvalue of the slow system diverging to infinity.

Summarizing, the following results have been proved in this section: (1) The singularity induced bifurcation in Σ_1 at $\mu_1 = 0$ arises as the limiting behavior (when $\epsilon \rightarrow 0$) of Hopf bifurcations in the singularly perturbed system Σ_{vP} ; (2) The oscillatory jump phenomena for $\mu_1 < 0$ and $\mu_2 > 0$ in Σ_1 with parasitic dynamics is "generated" by the singularity induced bifurcation in Σ_1 , as the limiting behavior of periodic orbits "generated" by Hopf bifurcations in Σ_{vP} ; (3) The stability of the periodic orbits and their size can be assessed from standard normal form computations at $\mu_1 = 0$. In other words, *oscillations in the van der Pol oscillator Σ_{vP} can be constructed from the singularity induced bifurcation in Σ_1* . In the next section, some of these results are generalized to the large system Σ_ϵ and its slow system Σ_s .

III. SINGULARITY INDUCED BIFURCATION IN THE LARGE SYSTEM Σ_ϵ

The problem studied in this section can be posed as follows: what is the generic behavior of the singularly perturbed system Σ_ϵ when the system equilibrium (9)–(10) is at the singular surface (11) upon some parameter variation? By restricting the analysis to the slow system Σ_s , this question has been analyzed in [6]–[8] and the result on the eigenvalues is summarized in the Appendix. More details on the geometry of the trajectories near the singularity induced bifurcation for Σ_s can be seen in [7], [8], [9].

The main result which relates the static conditions (9)–(10) to a dynamic property of Σ_ϵ namely the presence of purely imaginary eigenvalues is presented next. A single parameter (say μ) variation is considered for simplicity and the bifurcation point is assumed to be $(0, 0, \mu_0)$.

Corollary 1: Suppose the conditions (SI1), (SI2) and (SI3') of the Singularity Induced bifurcation Theorem (see Appendix) are satisfied for Σ_s . Suppose the following conditions are also satisfied at $(0, 0, \mu_0)$:

(SI4) All the $(n-1)$ bounded eigenvalues of J stay away from the imaginary axis.

(SI5) $D_y g$ does not have any purely imaginary eigenvalues.

(SI6) $b > 0$ ($b < 0$) when n_f is odd (even) where n_f is the number of eigenvalues of $D_y g$ with negative real parts.

Then given any parameter interval $(\tilde{\mu}_1, \tilde{\mu}_2)$ containing $\mu = \mu_0$, there exists an $\epsilon_0 > 0$ such that for any $\epsilon \in (0, \epsilon_0)$, the system Jacobian J_ϵ of Σ_ϵ ,

$$J_\epsilon = \begin{pmatrix} D_x f & D_y f \\ \frac{1}{\epsilon} D_x g & \frac{1}{\epsilon} D_y g \end{pmatrix} \quad (23)$$

evaluated along the equilibrium locus $EQ(\mu)$ has a pair of eigenvalues which cross the imaginary axis away from the origin, within the parameter interval $(\tilde{\mu}_1, \tilde{\mu}_2)$.

Proof: The proof follows from the SIB Theorem and from standard singular perturbation results [2] by simple $\epsilon-\delta$ type technical arguments. The basic idea in the proof is to show that for small $\epsilon > 0$,

the eigenstructure of the system Σ_ϵ at the equilibrium for some $\hat{\mu}_1$ and $\hat{\mu}_2$ differs by two eigenvalues, but zero crossings are ruled out, so the eigenvalue crossing must occur on the imaginary axis.

First note that the equilibrium locus $EQ(\mu)$ of Σ_s in the SIB Theorem is also the unique equilibrium locus for Σ_ϵ near $(0, 0, \mu_0)$. From linear algebra, we have $\det(J_\epsilon) = \epsilon^{-m} \det(J_1)$ where J_1 is the Jacobian in (SI2). Therefore (SI2) also implies that the Jacobian J_ϵ is nonsingular at $(0, 0, \mu_0)$ for any $\epsilon > 0$. Moreover since nonsingularity of a matrix is an open property (being an inequality condition), it follows that there exists an interval (μ_1, μ_2) containing μ_0 such that for all $\mu \in (\mu_1, \mu_2)$, the Jacobian J_1 evaluated along $EQ(\mu)$ is nonsingular. Again by linear algebra, this property holds for J_ϵ evaluated along $EQ(\mu)$ for all $\mu \in (\mu_1, \mu_2)$ and for all $\epsilon > 0$. In other words, the Jacobian J_ϵ does not have any zero eigenvalues along $EQ(\mu)$ for all $\mu \in (\mu_1, \mu_2)$ and all $\epsilon > 0$.

From the SIB Theorem, note that the eigenstructure of the slow system Jacobian J along $EQ(\mu)$ undergoes a change at $\mu = \mu_0$. Also note that the Jacobian of the fast system $D_y g$ is singular at $(0, 0, \mu_0)$ with exactly one zero eigenvalue and no other eigenvalues on the imaginary axis. Therefore by (SI1), (SI3') and (SI5), it follows that exactly one eigenvalue of the Jacobian $D_y g$ evaluated along $EQ(\mu)$ crosses the imaginary axis by passing through the origin. Therefore we can choose parameter values $\hat{\mu}_1 \in (\mu_1, \mu_2)$ and $\hat{\mu}_2 \in (\mu_1, \mu_2)$ on the two sides of $\mu = \mu_0$, arbitrarily close to $\mu = \mu_0$, so that the number of eigenvalues with negative real parts of the slow and fast Jacobians J and $D_y g$, evaluated at $EQ(\hat{\mu}_1)$ and at $EQ(\hat{\mu}_2)$, each differs by one. Next applying standard singular perturbation results [2] on the eigenvalues of Σ_ϵ , for $\mu \neq \mu_0$, since the Jacobians $D_y g$ and J do not have any eigenvalues on the imaginary axis, it follows that we can find small ϵ neighborhoods say $\hat{\epsilon}_i$ so that for $\mu = \hat{\mu}_i$, the eigenvalues of J_ϵ are close to those of the Jacobians J and $D_y g$ for $i = 1, 2$. Let ϵ_0 be the minimum of $\hat{\epsilon}_i$ for $i = 1, 2$.

Consider any $\epsilon \in (0, \epsilon_0)$. By construction, the Jacobian J_ϵ evaluated along $EQ(\mu)$ does not contain any zero eigenvalues for all $\mu \in (\hat{\mu}_1, \hat{\mu}_2)$. But the number of eigenvalues with negative real parts of J_ϵ at $\mu = \hat{\mu}_1$ differs from that at $\mu = \hat{\mu}_2$ by two (one each from the slow system Jacobian J and the fast system Jacobian $D_y g$). Here the condition (SI6) is crucial since it rules out the possibility of complementary crossings of the eigenvalues. That is, cases such as the eigenvalue of J moving from C^- to C^+ while the eigenvalue of $D_y g$ moves from C^- to C^+ with no net change in the overall eigenstructure of Σ_ϵ are ruled out by (SI6). To prove this, note that $\Delta(x(\mu), y(\mu), \mu)$ is the product of the eigenvalues of $D_y g$ evaluated along $EQ(\mu)$ and its derivative at $\mu = \mu_0$ is the constant c . Therefore the real eigenvalue of $D_y g$ which is zero at $\mu = \mu_0$ can be approximated as $(-1)^{n_f} \alpha c (\mu - \mu_0) + \mathcal{O}(\mu - \mu_0)^2$ for some $\alpha > 0$. Also the diverging eigenvalue of J from the SIB Theorem can be approximated as $\frac{b}{c(\mu - \mu_0)} + \mathcal{O}(\mu - \mu_0)^2$ [6]. Therefore the number of eigenvalues with negative real parts of J_ϵ at $\mu = \hat{\mu}_1$ differs from that at $\mu = \hat{\mu}_2$ by two.

Since the eigenvalues of J_ϵ along $EQ(\mu)$ continuously depend on μ and since Σ_ϵ is smooth for $\epsilon > 0$, it follows that there exists an imaginary axis crossing of the eigenvalues between $\hat{\mu}_1$ and $\hat{\mu}_2$. Since $\hat{\mu}_1$ and $\hat{\mu}_2$ can be chosen to be arbitrarily close to μ_0 , the results follows for any interval $\hat{\mu}_1, \hat{\mu}_2$ containing $\mu = \mu_0$. Q.E.D.

Remarks:

- 1) The conditions (SI1), (SI2), (SI3'), (SI4) and (SI5) being inequality constraints, are all generically satisfied for the stated problem, namely that of the equilibrium at the singularity (conditions (9)–(11)).
- 2) The condition (SI6) is a simplifying assumption which ensures that the critical eigenvalues of the slow and fast system either both move from C^+ to C^- or vice versa, together (as

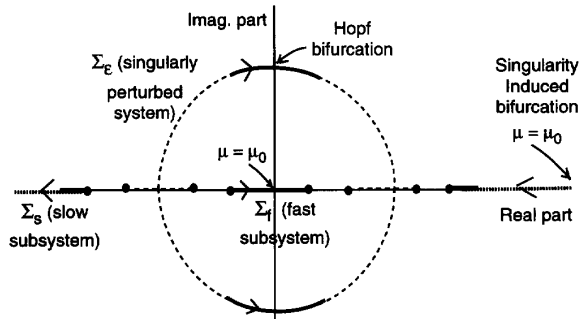


Fig. 2. Movement of the eigenvalues near the bifurcation.

shown in Fig. 2). For the practically interesting case, that is, when a stable equilibrium crosses the singularity, since all the eigenvalues of the slow and fast system lie in the complex left half plane before the bifurcation, indeed this condition is satisfied.

- 3) Basically the Corollary above relates a set of simple algebraic conditions (9)–(11) to an eigenvalue property of Σ_ϵ , specifically that the system Σ_ϵ contains purely imaginary eigenvalues close to the bifurcation point.
- 4) When a stable equilibrium of Σ_ϵ undergoes a SIB bifurcation, then after the bifurcation, two eigenvalues are in the right half plane, and these eigenvalues are one each of the slow system and the fast system. Interestingly in the slow system, the cross-over occurs at infinity, while in the fast system, the cross-over occurs at zero (see Fig. 2). In the actual singularly perturbed system Σ_ϵ , the two eigenvalues cross over across the imaginary axis away from the origin. This can be easily demonstrated, for instance, in the van der Pol example in Section 2 from (19). Moreover generically such eigenvalue crossings on the imaginary axis should lead to Hopf bifurcations, therefore the birth of limit cycles from the bifurcating equilibrium for Σ_ϵ . Normal form computations are necessary for concluding whether such Hopf bifurcations are supercritical or subcritical, and how these limit cycles behave when $\epsilon \rightarrow 0$. For simple examples such as the van der Pol oscillator, these computations can be carried out easily as shown in Section 2. But for large systems, it would be highly desirable to derive explicit formulas for such normal form coefficients so that they can be directly evaluated say from the slow system or the DAE system Σ_s . Intuitively since the bifurcating eigenvalues at the Hopf bifurcation are contributed one each by the slow dynamics and the fast dynamics, respectively, the oscillations should involve the interaction of the slow and fast dynamics, such as in the van der Pol example, thus leading to oscillatory jump phenomena.

IV. CONCLUSION

For the case of a van der Pol oscillator, it was proved that the oscillations are "generated" at the singularity induced bifurcation in its slow system which is the limit of Hopf bifurcations in the singularly perturbed models. For the general nonlinear system Σ_ϵ , under generic transversality conditions, it was proved that when a stable equilibrium undergoes the singularity induced bifurcation, the singularly perturbed system has purely imaginary eigenvalues near the bifurcation point. Generically such imaginary axis crossings should lead to Hopf bifurcations and the birth of limit cycles in the singularly perturbed models. More investigation is indicated for establishing

the geometry of the trajectories of Σ_ϵ near the singularity induced bifurcation.

APPENDIX

Theorem 1 (Singularity Induced Bifurcation Theorem) [6]–[9]: Consider the system Σ_s with a 1-dimensional parameter (say μ) space. Suppose the following conditions are satisfied at $(0, 0, \mu_0)$:

(SI1) $f(0, 0, \mu_0) = 0$, $g(0, 0, \mu_0) = 0$, $D_y g$ has a simple zero eigenvalue, and $D_y \text{fadj}(D_y g) D_x g$ has a nonzero eigenvalue

(SI2) $\begin{pmatrix} D_x f & D_y f \\ D_x g & D_y g \end{pmatrix}$ is nonsingular

(SI3') $\begin{pmatrix} D_x f & D_y f & D_\mu f \\ D_x g & D_y g & D_\mu g \\ D_x \Delta & D_y \Delta & D_\mu \Delta \end{pmatrix}$ is nonsingular.

Then there exists a smooth curve of equilibria, say $EQ(\mu) := (x(\mu), y(\mu), \mu)$ in R^{n+m+1} which passes through $(0, 0, \mu_0)$ and is transversal to the singular surface S at $(0, 0, \mu_0)$. When μ increases through μ_0 , one eigenvalue of the system, (i.e. an eigenvalue of

$$J = D_x f - D_y f (D_y g)^{-1} D_x g \quad (24)$$

evaluated along the equilibrium locus), moves from the open left half complex plane C^- to the open right half complex plane C^+ if $\frac{b}{c} > 0$ (from C^+ to C^- if $\frac{b}{c} < 0$) along the real axis by diverging through ∞ . The other eigenvalues remain bounded and stay away from the origin. Here c is defined as the derivative of Δ along $EQ(\mu)$

$$c := \frac{d}{d\mu}_{\mu=\mu_0} \Delta(x(\mu), y(\mu), \mu) \quad (25)$$

and b is defined as the only nonzero eigenvalue of $-D_y \text{fadj}(D_y g) D_x g$ at $(0, 0, \mu_0)$ where $\text{adj}(A)$ stands for the classical matrix adjoint of the matrix A .

Brief Outline of the Proof: Applying the implicit function theorem, there exists a unique equilibrium locus $(x(\mu), y(\mu), \mu)$ locally near $\mu = \mu_0$, since the relevant Jacobian is nonsingular at $(0, 0, \mu_0)$ from (SI2). Next conditions (SI2) and (SI3') can together be used to show that the determinant Δ is dominated by the linear term along the equilibrium locus, i.e.

$$c = \frac{d}{d\mu}_{\mu=\mu_0} \Delta(x(\mu), y(\mu), \mu) \neq 0 \quad (26)$$

which proves that the equilibrium locus $EQ(\mu)$ is transversal to the singularity S . When $\mu = \mu_0$, since the equilibrium is at the singular surface, Σ_s is not smooth near the singular equilibrium. To facilitate the analysis, a global extension of a singular transformation introduced in [4] can be used to construct a globally well-defined smooth transformed vector field called Z^T [6] and Z^T leaves L invariant. The key step in the proof is to connect the transversality conditions (SI1)–(SI3') with an eigenvalue property, namely that the smooth vector field Z^T has a unique nonzero eigenvalue (defined above as b) and $n - 1$ zero eigenvalues at $(0, 0, \mu_0)$. This argument combines the linear algebraic properties of the classical matrix adjoint from the construction of Z^T and the existence of a center manifold from the center manifold theory by carrying out certain standard center manifold computations. It can be shown that the singular vector field Σ_s is actually smooth when restricted to such a center manifold of Z^T which provides some insight into the geometry of trajectories

near $(0, 0, \mu_0)$ [7]–[9]. For our constrained system Σ_s , the eigenvalue corresponding to b of Z^T (say $\lambda_n(\mu)$) blows up along

$$\lambda_n(\mu) = \frac{b}{c(\mu - \mu_0)} + \mathcal{O}(\mu - \mu_0). \quad (27)$$

while the remaining $(n - 1)$ eigenvalues remain bounded which completes the proof. Q.E.D.

REFERENCES

- [1] L. O. Chua and A. C. Deng, "Impasse points-Part II: Analytical aspects," *Int. J. Circuit Theory*, 1989.
- [2] N. Fenichel, "Geometric singular perturbation theory for ordinary differential equations," *J. Differential Equations*, vol. 31, pp. 53–93.
- [3] R. E. O'Malley, *Singular Perturbation Methods for Ordinary Differential Equations*. New York: Springer-Verlag, 1991.
- [4] F. Takens, "Constrained equations: a study of implicit differential equations and their discontinuous solutions," in *Structural Stability, the Theory of Catastrophes and the Application in the Sciences, Lecture Notes in Mathematics*, Springer-Verlag, New York, 1976, pp. 143–234.
- [5] S. Sastry and C. Desoer, "Jump behavior of circuits and systems," *IEEE Trans. CSAS*, vol. 28, no. 12, Dec. 1981, pp. 1109–1124.
- [6] V. Venkatasubramanian, H. Schättler and J. Zaborszky, "A taxonomy of the dynamics of the large electric power system with emphasis on its voltage stability," in *Proc. NSF Int. Workshop on Bulk Power Syst. Voltage Phenomena-II*, 1991, pp. 9–52.
- [7] V. Venkatasubramanian, "A taxonomy of the dynamics of large differential-algebraic systems such as the power system," *Ph.D. thesis*, Washington University, St. Louis, MO, Aug. 1992.
- [8] V. Venkatasubramanian, H. Schättler and J. Zaborszky, "A stability theory of large differential algebraic systems—a taxonomy," *Report SSM 9201-Part I*, Department of Systems Science and Mathematics, Washington University, School of Engineering and Applied Science, Saint Louis, MO, Sept. 1992.
- [9] V. Venkatasubramanian, H. Schättler and J. Zaborszky, "Feasibility regions and bifurcation boundaries in constrained systems such as the large power system," submitted for publication.
- [10] A. K. Zvonkin and M. A. Shubin, "Non-standard analysis and singular perturbations of ordinary differential equations," *Russian Math. Surveys*, 39:2, 1984, pp. 69–131.
- [11] M. Diener, "The canard unchained or how fast/slow dynamical systems bifurcate," *The Math. Intelligencer*, vol. 6, no. 3, pp. 38–49, 1984.
- [12] E. Benoit, *Canards et enlacements*. Paris: Publications I.H.E.S., 1991.
- [13] J. Guckenheimer and P. Holmes, *Nonlinear Oscillations, Dynamical Systems and Bifurcations of Vector Fields*. New York: Springer-Verlag, 1983.
- [14] H. K. Khalil, *Nonlinear Systems*. New York: Macmillan Publishing Company, 1992.

Comments on "The Single CCH Biquads with High-Input Impedance"¹

Muhammad Taher Abuelma'atti

Attention is drawn to Fig. 7 of the above paper¹. The circuit will not operate if the two RC combinations are parallel connected as

¹S.-I. Liu and H.-W. Tsao, *IEEE Trans. Circuits and Syst.*, vol. 38, pp. 456–461, 1991.

Manuscript received April 27, 1994. This paper was recommended by Editor Martin Hasler.

The author is with King Fahd University of Petroleum and Minerals, Box 203, Dhahran 31261, Saudi Arabia.

IEEE Log Number 9405168.